



The Effect of Curve Cylinder Liner on in-Cylinder Tumble Flow Motion Characteristic using CFD Port Flow Simulation

Mohd Izamudin Itam Ahmed^{1,2,*}, Masri Baharom¹, Abd Rashid Abd Aziz¹

¹ Department of Mechanical Engineering, Universiti Teknologi PETRONAS (UTP), Bandar Seri Iskandar, Tronoh 32610, Perak, Malaysia

² Unit Teknologi Automotif, Kolej Komuniti Pasir Salak, Jalan Lebu Paduka, Changkat Lada, 36800 Kampung Gajah, Perak, Malaysia

ARTICLE INFO

Article history:

Received 11 April 2023

Received in revised form 14 May 2023

Accepted 11 June 2023

Available online 1 October 2023

Keywords:

In-cylinder flow; Curve Cylinder; ANSYS Fluent; Port Flow Simulation; RNG k- ϵ ; Crank-Rocker

ABSTRACT

One crucial task in determining maximum engine output performance is evaluating its respiration capacity. While the steady state flow bench is a commonly used tool in the automotive industry, computational fluid dynamics (CFD) provides a more detailed and comprehensive analysis of flow characteristics within the cylinder compared to experiments. The objective of this paper is to investigate the impact of curve cylinder liners on flow motion characteristics. Using both experimental and CFD methods, this study examines the effect of curve liners on tumble flow motion at different valve lifts and pressure differences. Scalar maps were analysed to understand the behaviour of flow, and the findings indicate that the air velocity measured at the intake port was consistent between both methods, permitting further CFD analysis. Results show that air velocity measured at the intake port was consistent between both methods, allowing for further CFD analysis. Differences in average velocities between liners were insignificant at lower valve lifts, but noticeable at higher valve lifts, with up to a 15.67% difference recorded when the curve wall assisted air flow, resulting in an increase in air rotational strength. In addition, curve liners produced 11.44% and 10.09% more turbulent kinetic energy (TKE) than straight liners for 150mmH₂O and 600mmH₂O, respectively, with Plane 2 exhibiting the most significant difference in average TKE. Finally, the tumble ratio produced within the curve cylinder was significantly higher than the slider cylinder liner, with differences of up to 17.03% and 11.04% found at higher valve lift (5.4mm) for 150mmH₂O and 600mmH₂O, respectively.

1. Introduction

Understanding the behavior of air flow characteristics in internal combustion engines (ICE) is crucial for designing engines efficiently. The intake and combustion strokes of normal 4-cycle engines, which are the initial two strokes, significantly impact the air flow pattern that enters the engine cylinder, affecting the performance of the ICE. Swirl and tumble flow models are commonly used to visualize flow generation [1]. Swirl flow involves the charge's rotation about the cylinder axis, while tumble flow involves a rotation orthogonal to the cylinder axis. Currently, engine manufacturers use steady state flow benches as standard to quantify engine breathing capabilities

* Corresponding author.

E-mail address: ccsmka@gmail.com (Mohd Izamudin bin Itam Ahmed)

based on intake port modification [2]. However, these methods cannot visualize the air flow pattern inside the cylinder.

A modification was made to steady state flow benches to accommodate measuring tools such as laser doppler anemometry (LDA), hot wire anemometry (HWA), and particle image velocimetry (PIV). LDA is fundamentally difficult and time consuming while HWA is an intrusive tool and very sensitive to ambient conditions thus may lead in providing inaccurate results. PIV on the other hand has successfully applied to the study of turbulent characteristics in recent years [3– 8].

A numerical method known as computational fluid dynamics (CFD) is an alternative approach that visualizes flow movements using numerical simulations [9– 12]. This method offers accurate results, detects design problems in the engine, and speeds up project processes while reducing costs compared to experimental methods. Several comparative studies have shown that CFD and experimental PIV methods give an accurate and reliable results [13– 17]. Additionally, CFD methods present an excellent opportunity to obtain detailed flow information about the entire flow field which is limited by PIV. Many turbulence models are available for simulation methods, and past research has shown that selective time-averaging turbulence models such as Renormalize Group (RNG) $k - \epsilon$ and Realizable $k - \epsilon$, $k - \omega$ SST are accurate depending on the experimental setup [18].

Heywood outlined the principle of port flow, where the engine geometry is held frozen without the piston crown to avoid backflow, and the valve lift and pressure difference can be varied as desired to simulate the turbulent flow generated [19]. However, El-Adawy *et al.*, investigated tumble motion evolution by introducing the piston crown and found agreement between PIV results and paddle wheel techniques [20].

In recent years, a team of researchers from University Teknologi PETRONAS (UTP) has developed toroidal engine designs with crank-rocker mechanisms. These engines have shown improved output characteristics when compared to conventional slider-crank engines [21– 23]. To achieve this, the researchers replaced the straight cylinder liner with a curve cylinder liner, while keeping the benchmark head cylinder of the Modenas ACE 115 engine. The curve-shaped liner was designed to reduce friction between the piston and cylinder walls, thus improving engine efficiency and increasing power output. Figure 1 displays the 3D model and fabricated Crank-Rocker Engines. [21].

Consequently, the objective of this paper is to investigate the effects of a curve cylinder liner on the generated tumble flow motion compared to a straight cylinder liner, using port flow simulation setup at different valve lifts and pressure differences under steady-state conditions. The analysis was conducted using commercial CFD tools with RNG $k - \epsilon$ as the turbulence model under standard operating conditions. The simulation data was compared between both liners in terms of average velocities, visualization of vorticity contours, average turbulence kinetic energy (TKE) and tumble ratio generated at specific tumble planes.

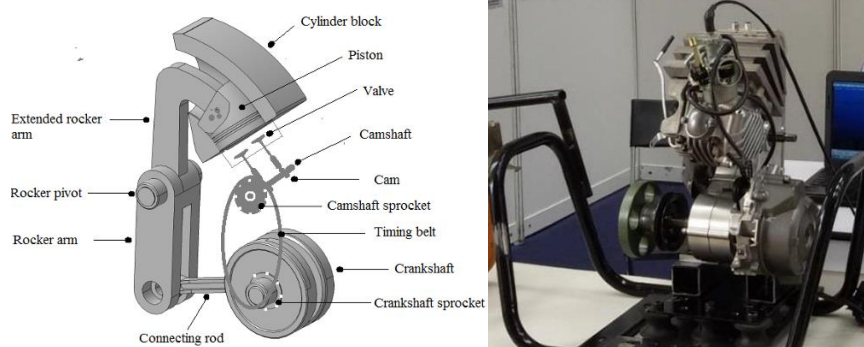


Fig. 1. 3D Model of Crank-Rocker Engine (left) and Assembled Crank-Rocker Engine (right) [21]

2. Methodology

2.1 Geometries Description

The current study involved the manufacturing and 3D CAD modelling of two-cylinder liners using CATIA V5 software. The specifications for the Slider and Crank-Rocker Engine were obtained from Table 1 in the UTP Researcher paper [21– 25]. To investigate the tumble motion inside the cylinder, the geometry of the liners was modified based on the method used by El-Adawy [3]. The piston face of both liners was designed to be located at the same distance as the engine stroke (50.6mm). In addition, outlet flow ports were incorporated on both sides of the liners to analyse the port flow. These outlet flow ports were positioned at 57% from Top Dead Centre (TDC) and were set to be 35% of the total bore in diameter. Figure 2 illustrates the two geometries of the cylinder liners.



Fig. 2. Model of (left) Straight Cylinder Liner and (right) Curve Cylinder Liner

Table 1

Specification of Slider and Crank-Rocker Engine [21– 25]

Parameter	Crank-rocker	Slider-crank
Bore	55mm	55mm
Stroke	50.6mm	50.6mm
Throw angle	21 ⁰	-
Cylinder Head Type	Hemisphere roof	Hemisphere roof
Maximum Valve Lift	5.4mm	5.4mm
Inner Seat diameter of intake valve	25mm	25mm
Valve seat angle	45 ⁰	45 ⁰

2.2 Experimental Setup

The steady-state flow bench is a commonly used tool in industry to measure volumetric efficiency, engine breathing capabilities, and air velocities. It is a cost-effective and non-intrusive method compared to other measurement tools, although the data on air flow rates are limited and may be affected by valves and intake port modifications. To accommodate both cylinders in the same setup for this study, the steady-state flow bench was modified by constructing an acrylic box with the cylinder head mounted on top of it. To ensure air was drawn from the intake port, a weighted load was placed on the cylinder head. Stepper motors were used to apply pressure differences of 150 and 600 mmH₂O, and the intake valve lift was adjusted using a micrometer custom holder, ranging from

1 mm to a maximum valve lift of 5.4 mm for both designs, with increments of 1 mm at each pressure difference. The pressure difference of 600 mmH₂O was selected to ensure fully turbulent flow condition. The schematic for the steady-state flow bench is depicted in Figure 3. Air was drawn through the centrifugal compressor, the cylinder head, intake port, cylinder liner. An anemometer was placed before the inlet port to measure air velocity at the inlet during each case. The sucked air flow, which corresponds to the pressure drops generated inside the cylinder liner, was adjusted using a stepper motor and measured between the inner cylinder liner and ambient using a manometer.

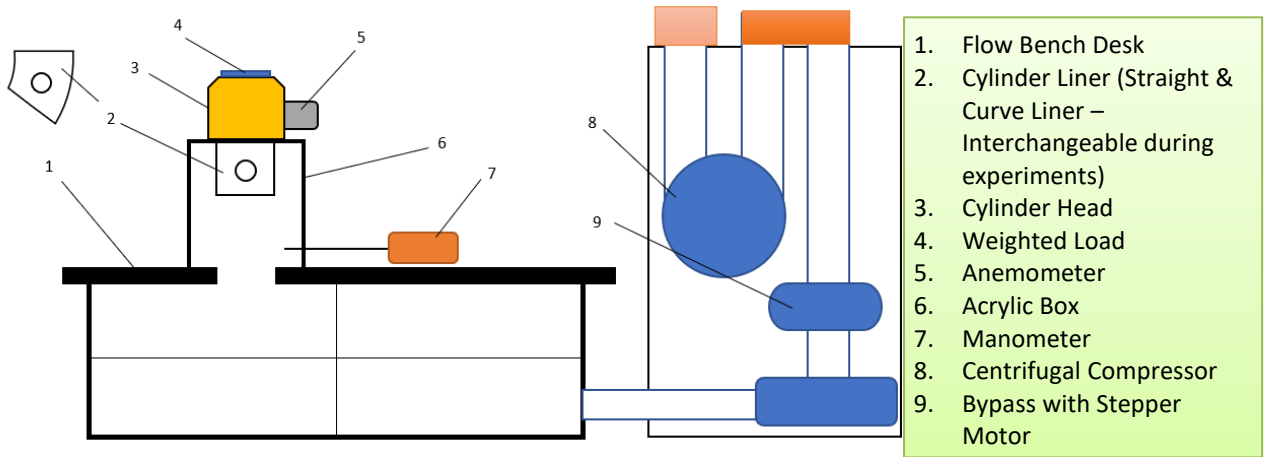


Fig. 3. Schematic of modified Steady State Flow Bench

2.3 CFD Simulation Setup

To conduct the port flow simulations, the commercial software ANSYS was utilized. The initial modelling of the cylinder head and cylinder liners was carried out using CATIA V5 software. Subsequently, these models were imported into ANSYS Workbench and ANSYS Fluent for further processing and solving. The 3D geometry models were then divided into four main parts, namely the inplenum region, port valve, combustion chamber, and outplenum region, as illustrated in Figure 4. Each part was assigned a specific mesh type based on its external domain shape, utilizing the difference meshing method. The upper cylinder head region was meshed using tetrahedral types, while the chamber and outplenum region were meshed using hex/prism mesh types. Furthermore, inflation layers were applied to all parts to accurately capture the near-wall region.

2.3.1 Governing equation

The operating conditions inside internal combustion engines are inherently turbulent. To numerically calculate the flow generated within the engine cylinder, whether in cold-flow or port flow simulation, Navier-Stokes equations can be utilized. The equations for incompressible flows describe the conservation of mass, momentum, and energy of a fluid with constant density, and can be succinctly described as follows:

Continuity equation:

$$\frac{\partial \rho}{\partial t} + \nabla \cdot (\rho u) = 0 \tag{1}$$

Momentum equation:

$$\rho \left(\frac{\partial u}{\partial t} + u \cdot \nabla u \right) = -\nabla p + \nabla \cdot \tau + \rho g \quad (2)$$

Energy equation:

$$\rho \left(\frac{\partial e}{\partial t} + u \cdot \nabla e \right) = -p \nabla \cdot u + \nabla \cdot (k \nabla T) + \tau \cdot \nabla u + Q \quad (3)$$

where ρ is the density of the fluid, u is the velocity vector, p is the pressure, τ is the deviatoric stress tensor, g is the acceleration due to gravity, e is the internal energy per unit mass, k is the thermal conductivity, T is the temperature and Q is the rate of internal heat generation per unit volume.

To accurately account for turbulence, which is crucial in port flows, additional turbulence models such as the k-epsilon model and its variants, for this study RNG k-epsilon, can be incorporated alongside the Navier-Stokes equations. These models provide supplementary equations that characterize the turbulent fluctuations in the fluid and the turbulent viscosity. The turbulent viscosity is then used in the Navier-Stokes equations to accurately represent the effects of turbulence. This can be expressed mathematically as follows:

Turbulent kinetic energy equation

$$\frac{\partial}{\partial t} (\rho k) + \nabla \cdot (\rho u k) = \nabla \cdot (\mu_{eff} \nabla k) + Pk - \rho \varepsilon \quad (4)$$

Dissipation rate equation:

$$\frac{\partial(\rho \varepsilon)}{\partial t} + \nabla \cdot (\rho u \varepsilon) = \nabla \cdot (\mu_{eff} \nabla \varepsilon) + \frac{C_{1\varepsilon} C_{3\varepsilon}}{k \rho P\varepsilon} - \frac{C_{2\varepsilon} \rho \varepsilon^2}{k} \quad (5)$$

where k is the turbulent kinetic energy, ε is the rate of dissipation of turbulent kinetic energy, μ_{eff} is the effective viscosity, Pk is the production of turbulent kinetic energy and $C_{1\varepsilon}$, $C_{2\varepsilon}$, $C_{3\varepsilon}$ are model constants.

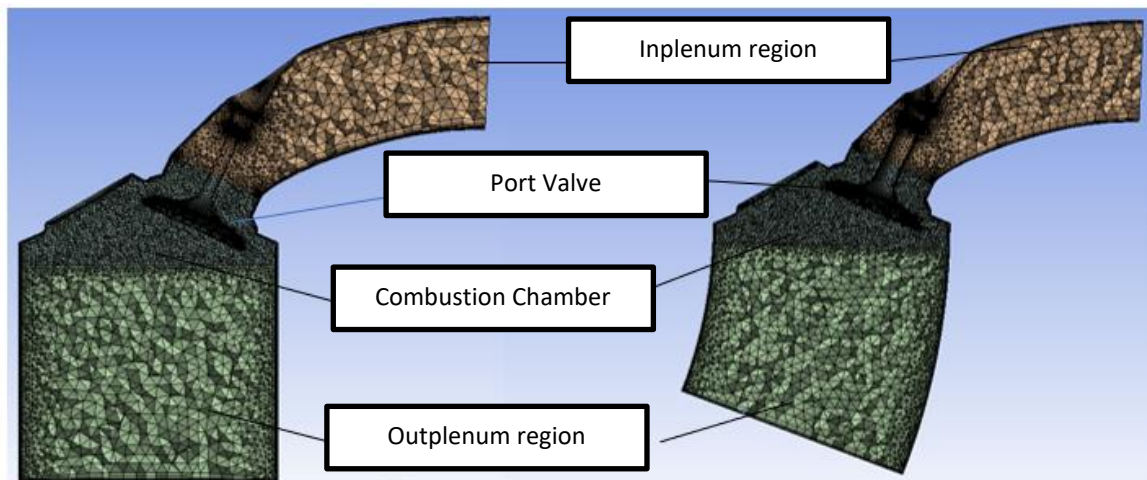


Fig. 4. Mesh Type with Inflation layers treatment for near wall region (left) Straight Cylinder Liner (right) Curve Liner

2.3.2 Mesh independent test

In the analysis of compressible flow problems, the quality of the mesh plays a critical role. To ensure accuracy, a mesh-independent test was conducted to determine the minimum mesh element required without increasing computational time and memory usage. Meshing variance, which refers to the face sizing of elements, was applied to the entire geometry while maintaining the mesh type in each region. During the simulation of the mesh-independent test, the intake valve lift was set to a maximum of 5.4mm with a pressure drop of 600 mmH₂O to simulate the maximum turbulence effect on each mesh setting. The maximum velocity generated was measured at one outlet, while the air velocity at the intake was obtained from steady-state experiments, as illustrated in Table 2.

Table 2
Mesh Criteria

Mesh	No of Elements	Face Sizing (mm)	Max Velocities at Outlet (ms ⁻¹)
Coarse	170875	3.5	25.69
Intermediate	207613	2.5	31.38
Fine	492492	1.0	30.51

Based on the results shown in Figure 5, it is evident that there is a significant difference in air velocities at the outlet for different mesh settings. The difference in data between coarse mesh and intermediate mesh is quite high, while the difference between intermediate and fine mesh is negligible. Therefore, to avoid increasing simulation time and cost, an intermediate mesh with 207,613 elements was selected since it can produce results as close as the fine mesh with 492,492 elements.

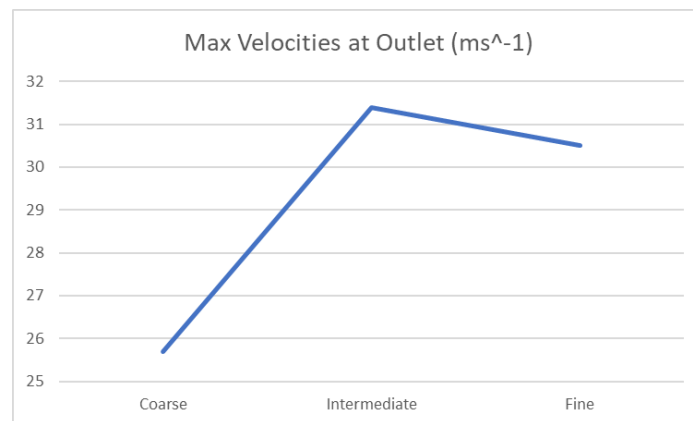


Fig. 5. Mesh Independent Test

2.3.3 Boundary conditions and initial values

The experimental design used in this analysis is based on steady-state flow, where pressure measurements were taken at the inlet and outlet of the model. Specifically, two outlet pressure conditions were used: -1471Pa (equivalent to 150mmH₂O pressure drop) and -5884Pa (equivalent to 600mmH₂O pressure drop). In addition, the wall temperature of all regions in the model was set to 297K. All constant parameters within ANSYS Fluent were set to their default values.

2.3.4 Turbulence models

Several turbulence models are commonly used in predicting in-cylinder turbulence flow studies based on literature [18]. In this study, the RNG k- ϵ model was selected due to its improved accuracy for swirling flows, which is relevant for this study as the outlet port is perpendicular to the target tumble planes, indicating the generation of swirling motion [26]. The simulation settings specified the turbulence method with turbulent intensity set at 2%, based on the Reynolds number and hydraulic diameter of 55mm.

2.3.5 Location of tumble plane

Two tumble planes were selected to characterize the effect of curve cylinders on flow motion across different valve lifts and pressure differences in this study. The planes were located mid-cylinder mid-valve ($x=0\text{mm}$, coloured in grey, referred to as *Plane 1*) and at the edge of the intake valve ($x=12.5\text{mm}$, coloured in green, referred to as *Plane 2*) as depicted in Figure 6. The upper limit of each plane was set at TDC ($z=0$), while the remaining plane limit followed the cylinder geometry. No further analysis was conducted within the cylinder head chamber dome since no significant differences in air velocities were found there due to same cylinder head used. ANSYS CFD-Post was used to analyse all the results. Velocity vector and scalar maps were generated initially, together with the results of average velocities at corresponding planes. Vorticity contours were obtained from all cases to provide an overview, visualization, and understanding of the flow behaviours inside different cylinder liners. Later, the average turbulent kinetic energy (TKE) and tumble ratio in each plane was calculated at every valve lift for each case.

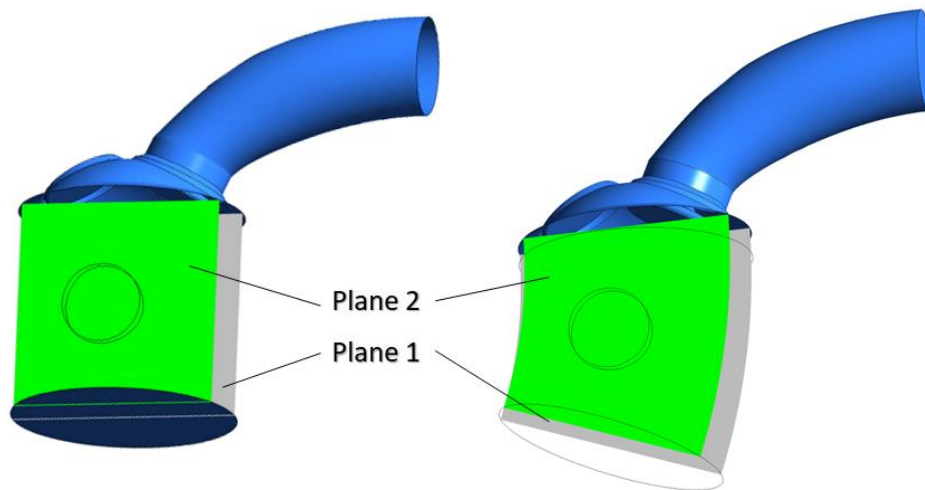


Fig. 6. Location of tumble planes for both liners

3. Results

3.1 Measured Air Velocity at Intake Port

The air velocity measurement obtained from the steady-state flow bench at the intake port was compared to simulation data, as indicated in Table 3. The results indicate that there was no significant difference observed between the straight and curve liners in both cases. The experimental data produced consistent results for both liners, suggesting that the cylinder liner geometry does not significantly impact the engine's breathing capacity, as both liners use the same cylinder head.

Although there was a slight variation in the simulation results, the difference was negligible, with a maximum difference of 1.96% between the experimental and simulation results.

Table 3
 Air velocities measured at intake port for each case (ms^{-1})

Pressure Difference (mmH_2O)	Valve Lift (mm)	Air Velocity measured at intake (ms^{-1})			
		Straight Liner (Flow Bench)	Curve Liner (Flow Bench)	Straight Liner (CFD)	Curve Liner (CFD)
600	5.4	39.9	39.9	40.11	39.74
	4	35.1	35.1	35.06	34.95
	3	27.1	27.1	27.22	27.09
	2	17.7	17.7	17.72	17.84
	1	9.2	9.2	9.14	9.16
150	5.4	20.2	20.2	20.48	20.34
	4	17.7	17.7	17.86	17.60
	3	13.7	13.7	13.80	13.79
	2	8.9	8.9	9.03	9.06
	1	4.5	4.5	4.59	4.59

3.2 Simulation Result

3.2.1 Velocity vector & scalar maps

In Figure 7, the average air velocities at different planes, including the outlet port, are compared. The velocities were calculated by taking the area-weighted average of the velocity magnitude in all components. The results show that the average velocity is negligible at lower valve lifts for all cases across pressure differences and valve lifts. However, there are significant differences at higher valve lifts. In the 600 mmH_2O cases, the average velocity at plane 1 is almost the same for both liner types. However, as the air moves towards the outlet ports through plane 2, the curve liner geometry accommodates more flow motion compared to the slider liner, resulting in a difference of 15.67% at 5.4mm valve lift. Since the average air velocity at the intake port is similar between liners, the same applies to the outlet ports. In the 150 mmH_2O case, the average air velocity at plane 1 is higher, especially at higher valve lifts, with differences of 12.9% and 14.28% between liners at 4mm and 5.4mm, respectively. Therefore, it can be concluded that the curve cylinder liner geometry induces air velocity more effectively at lower pressure differences.

Figures 8 and 9 provide a comparison of velocity vectors and scalar maps between the straight and curve liners at different valve lifts and pressure differences at plane 1 and plane 2, respectively. The scalar maps show that the air flow coming from the intake port through the intake valve separates into two main air jets, with the left side located near the exhaust valve having a higher air velocity. This is due to the curve liner geometry accommodating the air jets direction better. However, there are noticeable differences on the right side of the air jets, where the curve liner geometry assists the flow motion better in dispersing higher air velocity towards central region of the cylinder, especially at lower pressure differences with higher intake valve opening. Plane 2 recorded higher air velocity and better spreading streamlines based on scalar maps. At lower valve lift, where the air flow was highly restricted, and there was not much difference across all cases.

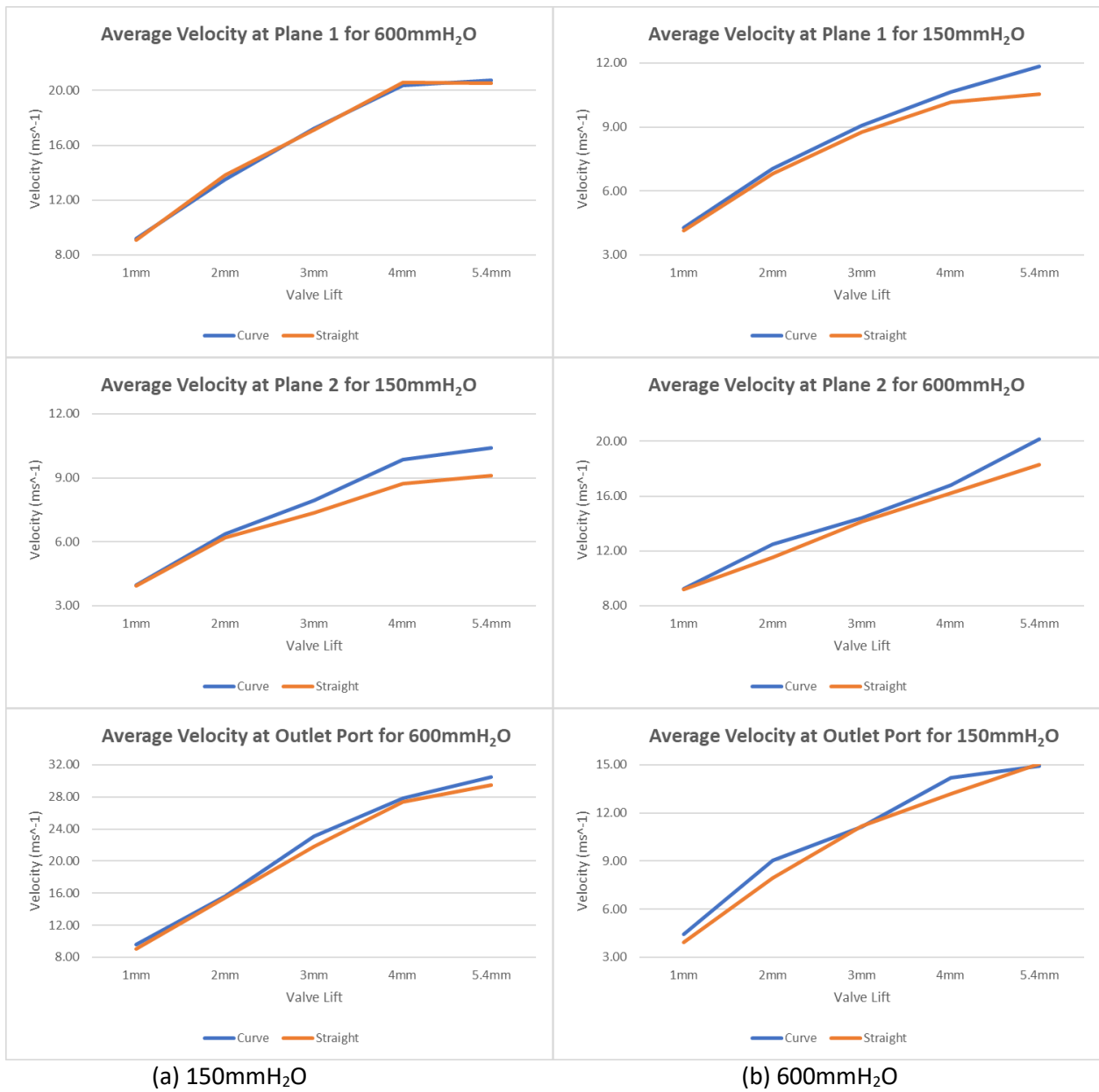


Fig. 7. Average Velocity at Plane 1, Plane 2 and Outlet Port for both liners (a) 150mmH₂O (b) 600mmH₂O

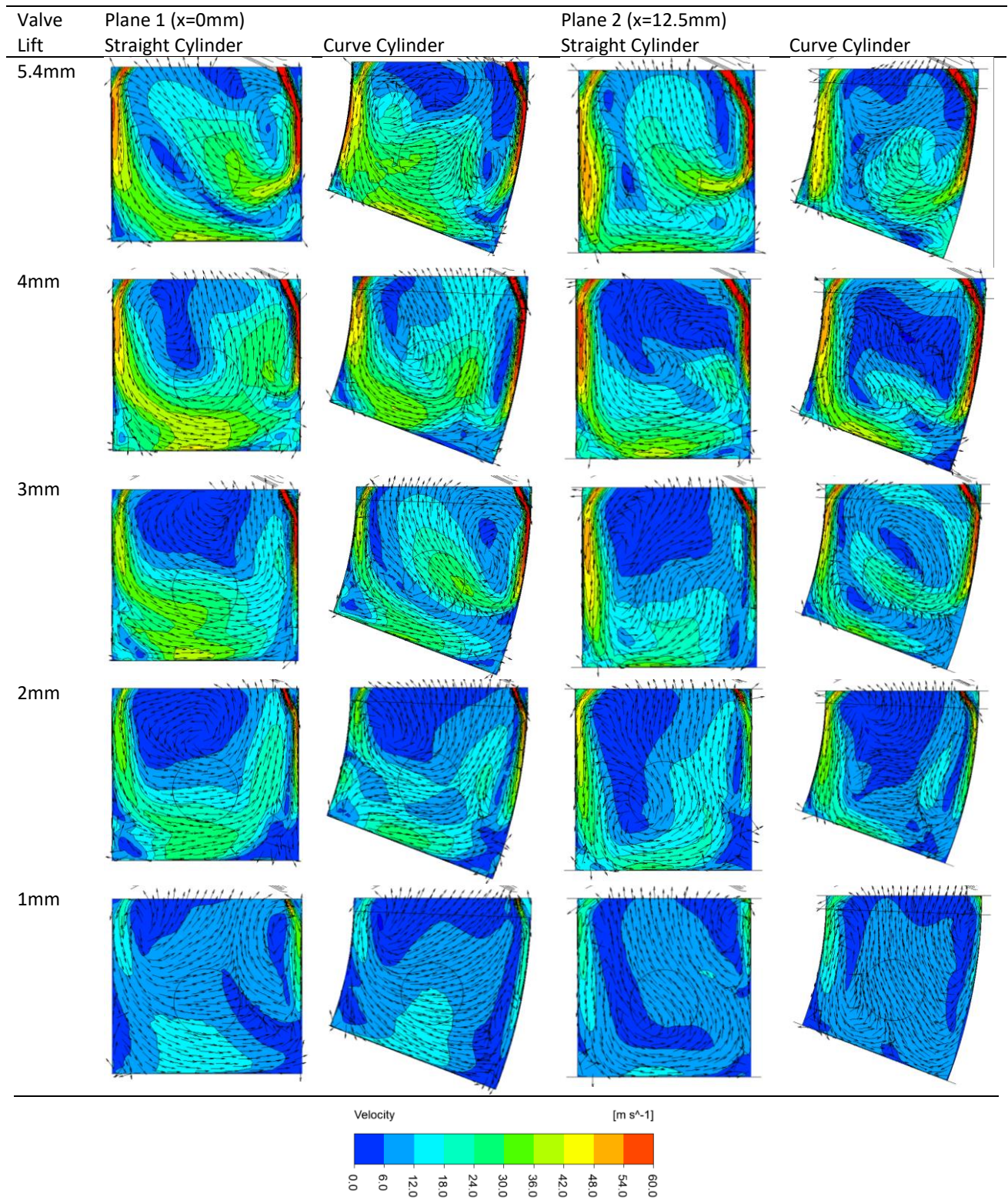


Fig. 8. Comparison of velocity vector and scalar maps for both liners at 600mmH₂O (Plane 1 & 2)

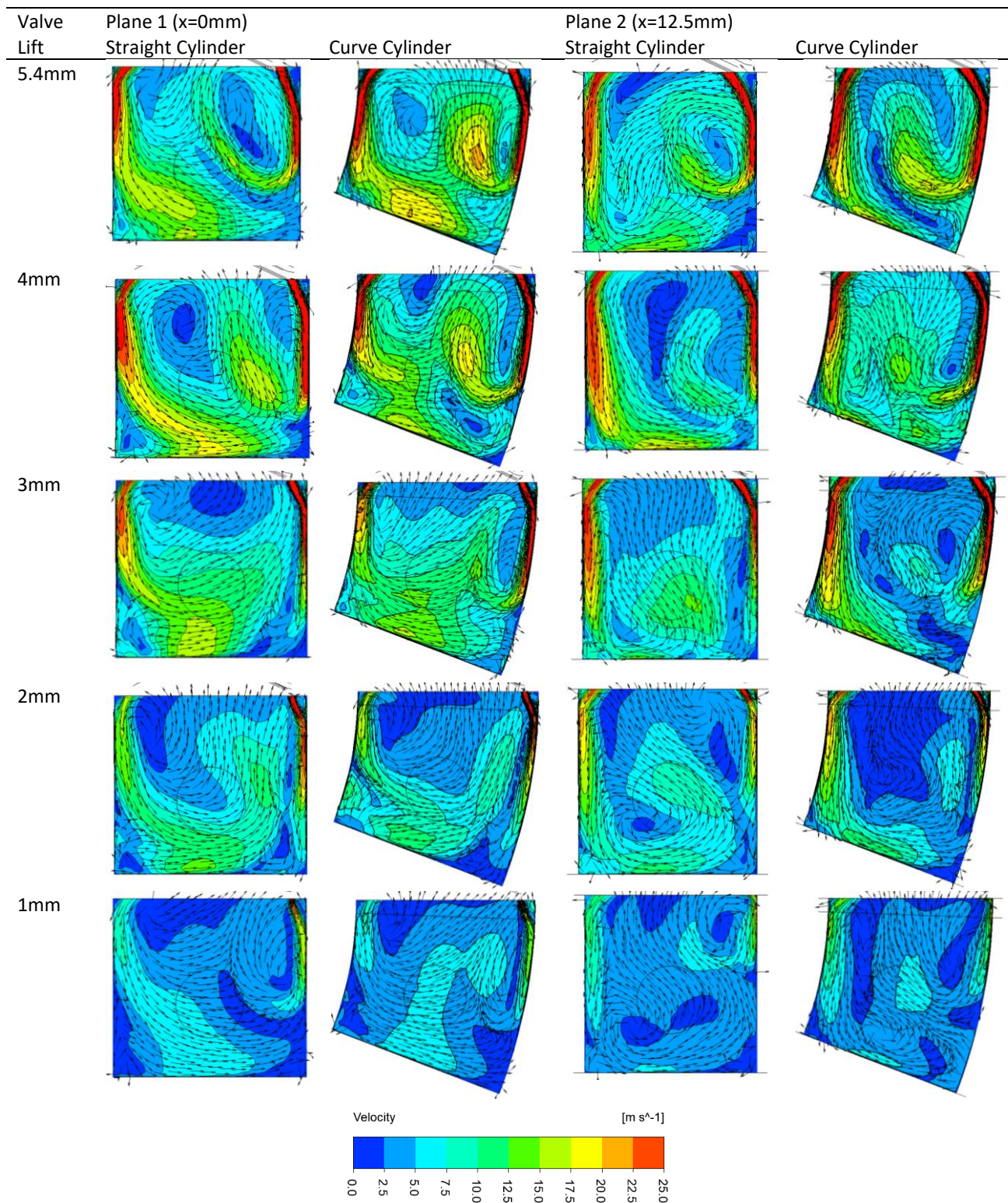


Fig. 9. Comparison of velocity vector and scalar maps for both liners at 150mmH₂O (Plane 1 & 2)

3.2.2 Turbulent Kinetic Energy (TKE)

In this study, turbulent kinetic energy (TKE) is used as a quantitative measure of turbulence intensity for a given flow. Higher valve lift and pressure difference generally result in higher TKE values, indicating greater energy and more effective fuel-air mixing. TKE is computed from the root mean square (RMS) of velocity vector fields using the following equation [29]:

$$TKE = \frac{1}{2} \rho V_{rms}^2 = \frac{1}{2} \rho (u_{rms}^2 + v_{rms}^2 + w_{rms}^2) \quad (6)$$

where u_{rms} , v_{rms} and w_{rms} are the RMS velocity components in the x, y and z directions respectively, and ρ is the air density.

Figure 10 presents the average weighted area of TKE values for each liner across all cases. Significant differences were observed at lower valve lifts and higher-pressure differences between planes 1 and 2. This is likely due to the curve cylinder geometry playing a more significant role in generating TKE as air rushes towards the outlet port. In general, the curve cylinder produces more average TKE at plane 2, with differences of up to 11.44% (at 150mmH₂O) and 10.09% (at 600mmH₂O) at lower valve lift. The differences of 6% to 7% in average TKE for both liners recorded at higher valve lifts favouring curve cylinder liners. It is interesting to note that larger difference found as high as 23.44% and 35.89% in 4mm and 2mm for 150mmH₂O and 600mmH₂O, respectively. Figures 11 and 12 show the comparison of TKE in terms of scalar maps for both liners at Plane 1 and Plane 2.

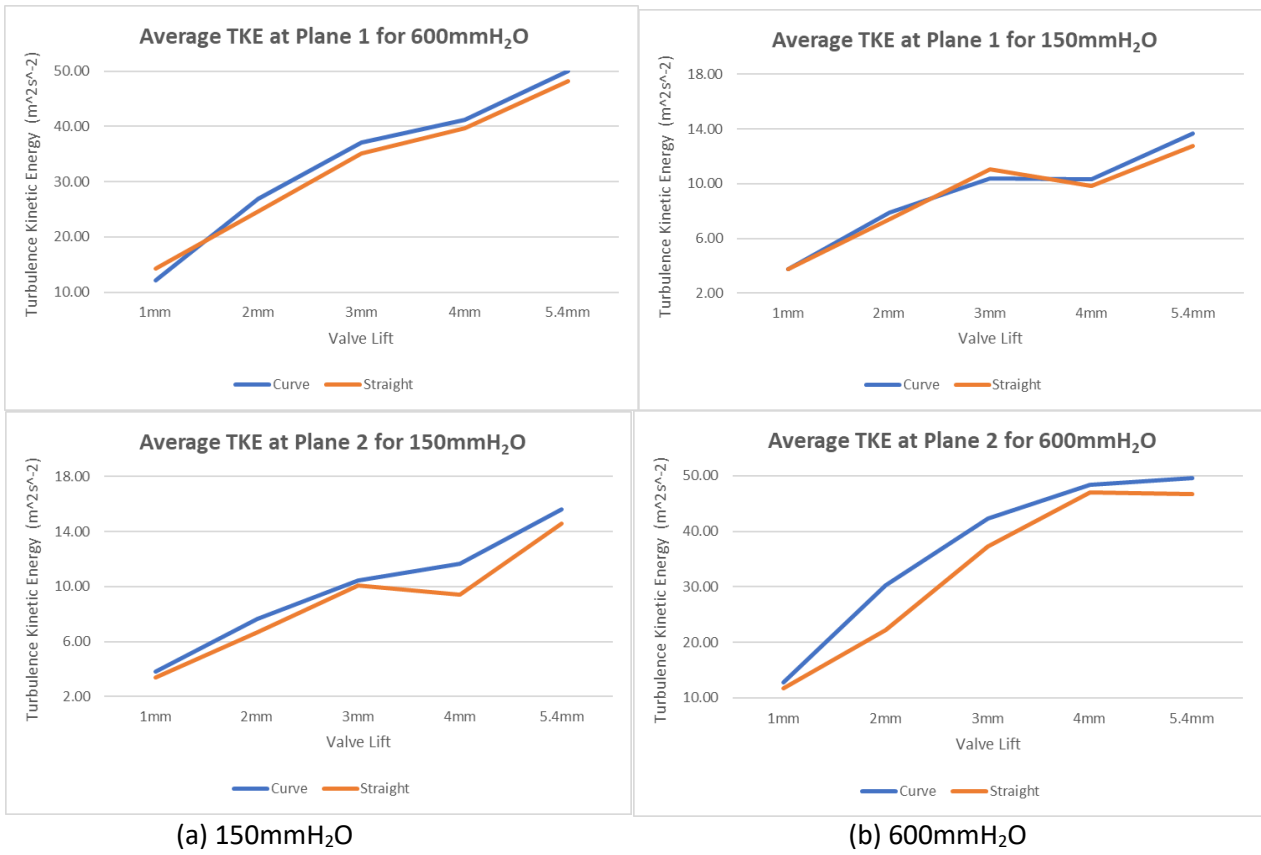


Fig. 10. Average TKE at Plane 1 and Plane 2 for both liners (a) 150mmH₂O (b) 600mmH₂O

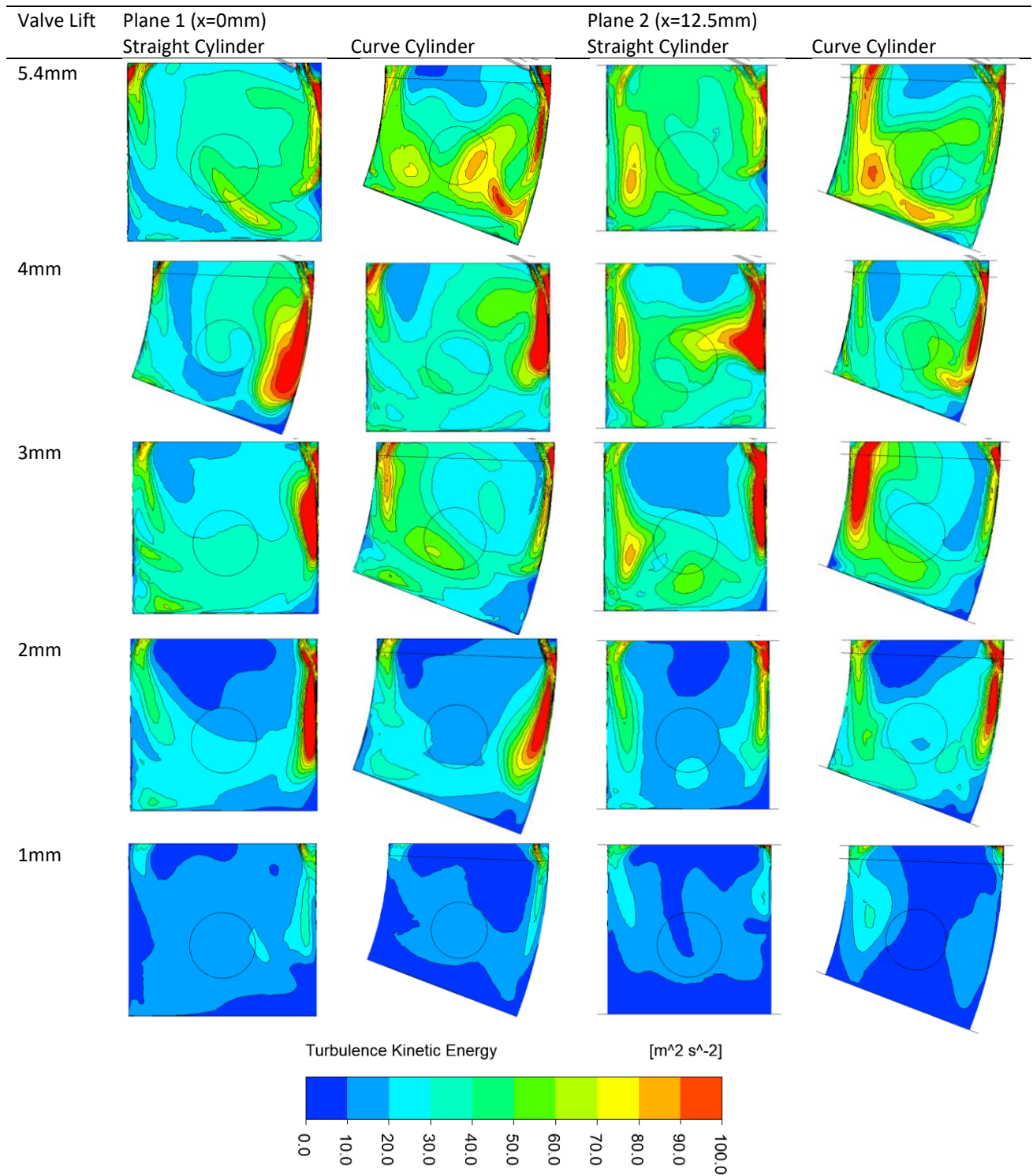


Fig. 11. Comparison of turbulent kinetic energy scalar maps for both liners at 600mmH₂O (Plane 1 & 2)

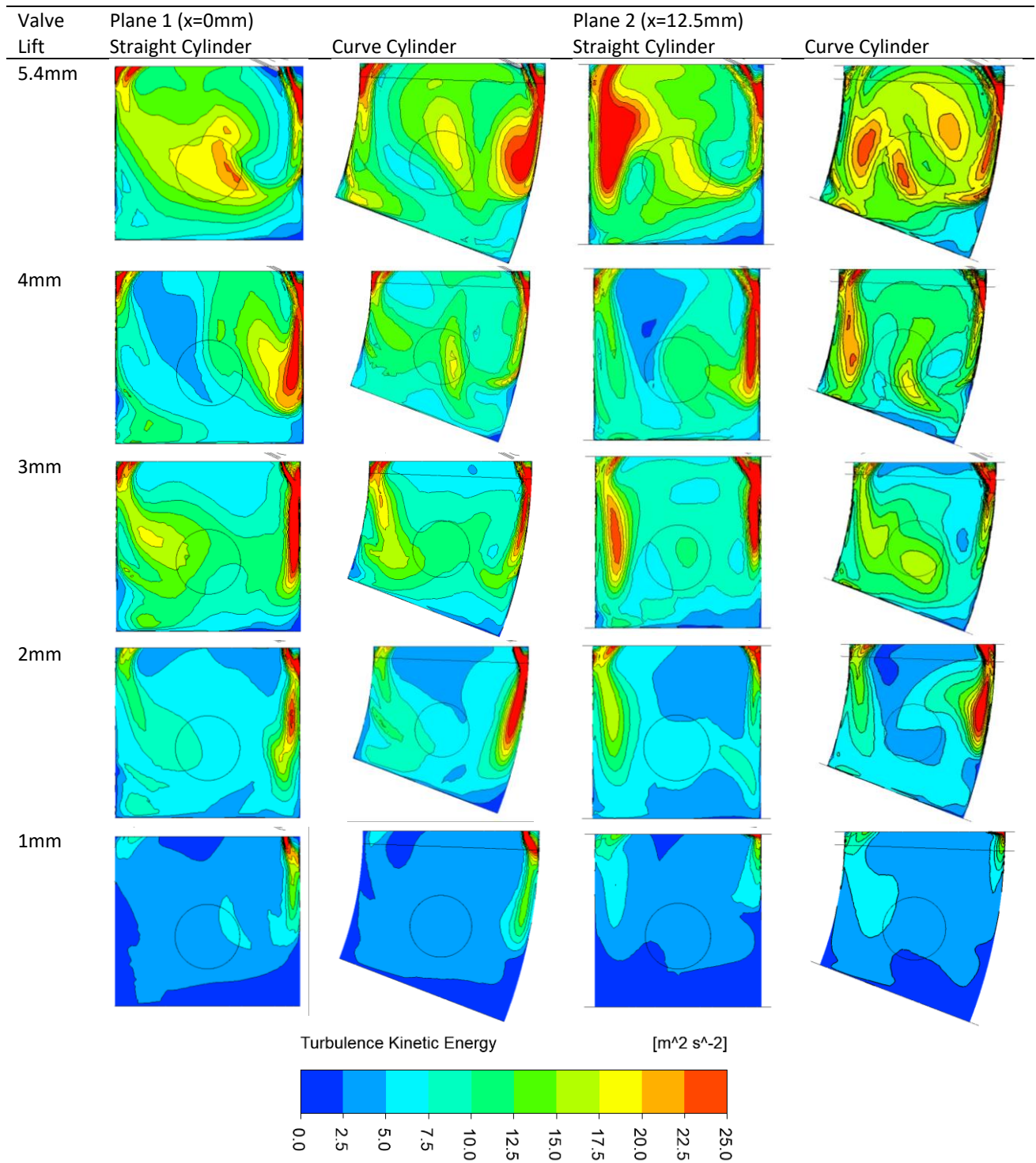


Fig. 12. Comparison of turbulent kinetic energy scalar maps for both liners at 150mmH₂O (Plane 1 & 2)

3.2.3 Vorticity

Vorticity is a measure of the local fluid rotation within the cylinder, specifically in the target plane of analysis. It is defined as the velocity curl and is often used to quantify the level of in-cylinder turbulence through the strength of fluid rotation per second, which has a significant impact on the engine's combustion process [27, 28]. CFD software is commonly used to calculate vorticity by simulating the airflow within the engine and providing detailed information on the velocity and direction of the fluid motion. The mathematical expression for vorticity is as follows:

$$\text{curl}(v) = \nabla \times v \quad (7)$$

where v is the velocity vector field, and $\nabla \times v$ is the curl of v .

Figure 13 and 14 presents a comparison of the vorticity scalar maps between the curve and straight cylinder liners at plane 1 and plane 2 respectively. The findings indicate that both liners exhibit higher vorticity strength under higher pressure differences. At lower valve lifts, both liners display lower rotational strength, but at higher valve lifts, the curve cylinder liner generates more strength compared to the straight cylinder liner. The curve wall amplifies the rotational strength of the air jets entering the cylinder liners and directs them towards the piston crown in efficient manner, that can be seen in the 600mmH₂O cases.

3.2.4 Tumble ratio

Tumble ratio (TR) is a dimensionless parameter that quantifies the degree of tumble motion in an engine cylinder. There is multiple definition of TR exist within literature. In this study, the TR was determined using the vorticity value since the simulation did not involve any moving parts, and only focuses on specific target planes making the conventional formula unsuitable. Mathematically, the TR is calculated as the area-weighted average of the vorticity at target planes, normalized by twice the crank angle speed, ω_e [20, 28] and can be expressed as:

$$TR = \frac{\omega_{AVG}}{2 \cdot \omega_e} \quad (8)$$

$$\omega_{AVG} = \frac{1}{A} \int_A \left| \frac{du_z}{dy} - \frac{du_y}{dz} \right| dA \quad (9)$$

$$\omega_e = \frac{4 \cdot \dot{m}}{\rho \cdot D^2 \cdot S} \quad (10)$$

where $\omega_{x\text{ AVG}}$ is mean vorticity in target plane, which located at x-component, \dot{m} is measured mass flow rate, ρ is air density, D is cylinder bore and S is cylinder stroke.

Figure 15 illustrates the tumble ratio calculated from Eq. (8) for all cases. In general, tumble ratio is increasing due to effect of valve lift and pressure differences [27]. The effect of curve cylinder liner is noticeable starting at lower valve lift, with difference of 5.99% and 7.86%. Moreover, the larger differences of 17.03% and 11.04% were recorded at higher valve lift (5.4mm) for 150mmH₂O and 600mmH₂O, respectively. This is due to the effect from curve cylinders towards air flow motion.

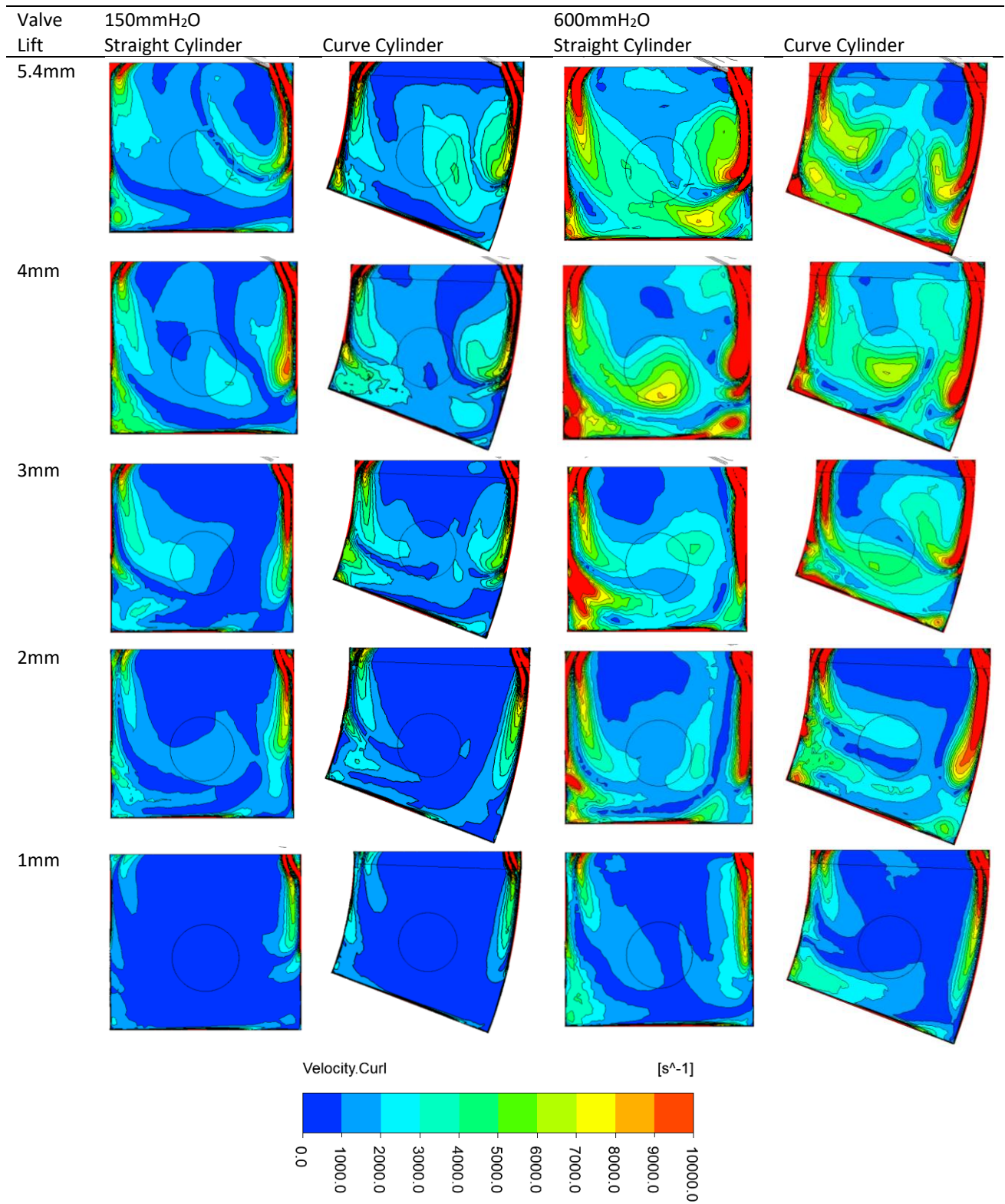


Fig. 13. Vorticity Contours at Plane 1 for both liners

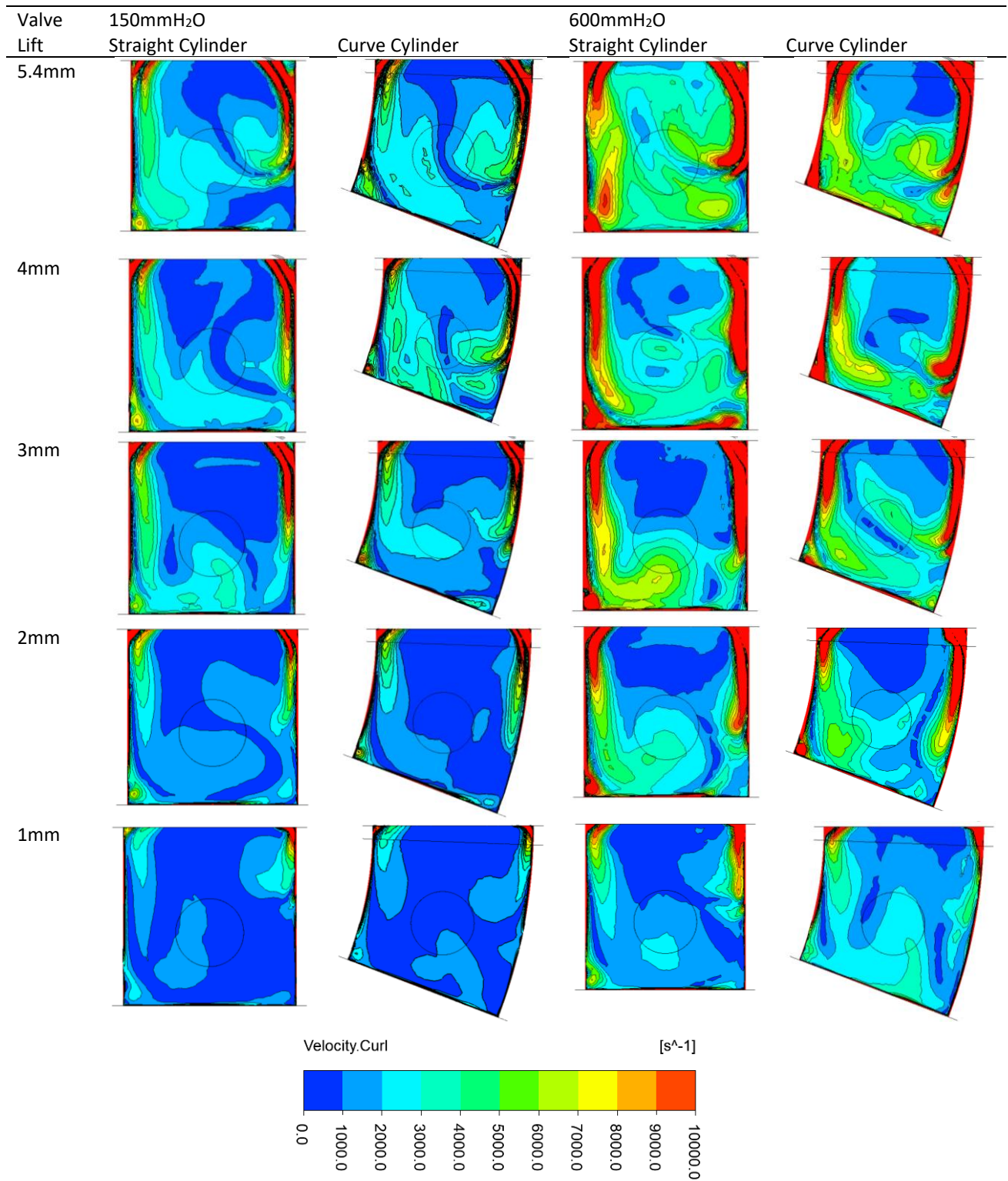


Fig. 14. Vorticity Contours at Plane 2 for both liners

It is noteworthy that there is a reduction in the tumble ratio for a valve lift of 2mm in the curve cylinder liner, across all cases. However, this reduction is compensated for by the significant improvement in higher valve lifts. Overall, these findings suggest that a curve cylinder liner can promote higher tumble ratios, which are desirable for efficient combustion in internal combustion engines.

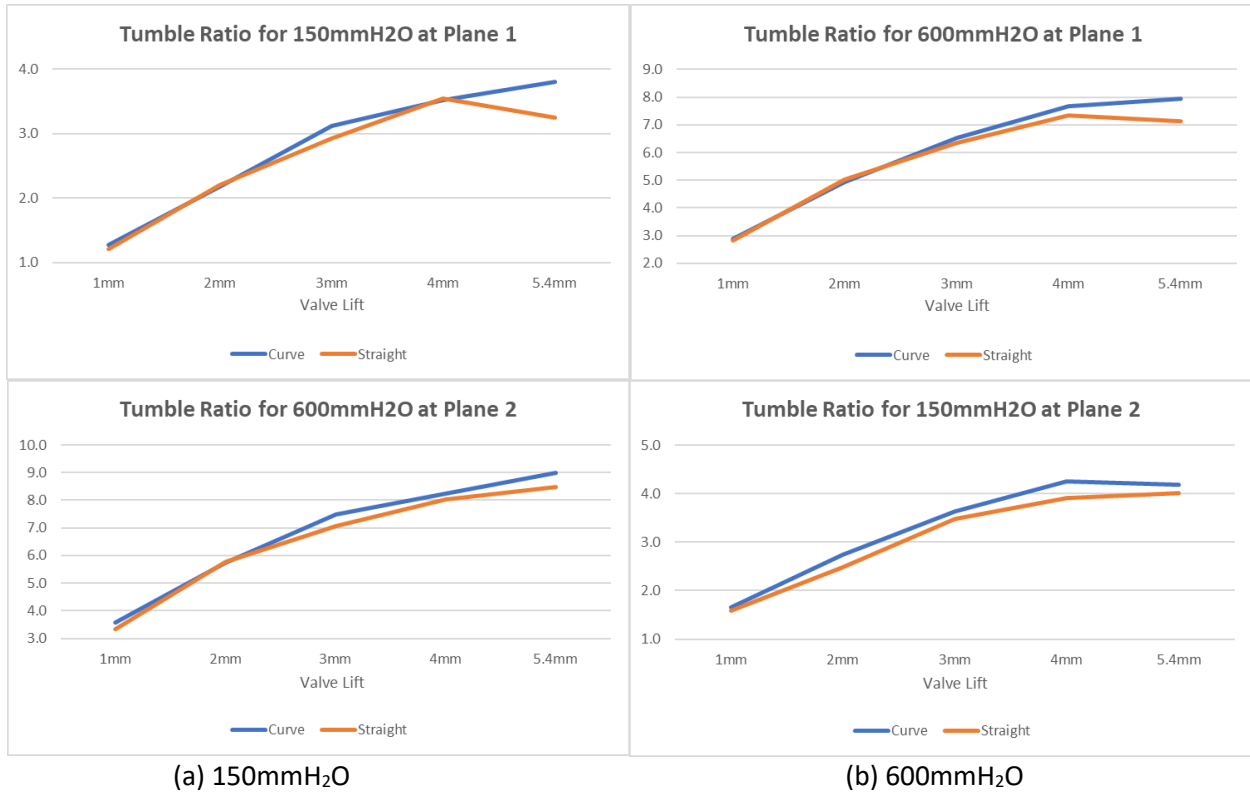


Fig. 15. Tumble Ratio at plane 1 and plane 2 for both liners (a) 150mmH₂O (b) 600mmH₂O

4. Conclusions

The effect of curve cylinder liners on the tumble flow motion generated at different valve lifts and pressure differences was investigated using experimental steady-state flow bench and CFD port flow simulation. Scalar maps for at mid-cylinder mid-intake valve (plane 1) and at the edge of the intake valve (plane 2) were obtained and analysed to understand the flow motion characteristics and their behaviour. The following conclusions can be drawn:

- i) The measured air velocity at the intake port is in agreement between both steady-state flow bench experiments and CFD simulations, with a maximum difference of 1.96% across all cases. Hence, the CFD simulation results can be used for further analysis.
- ii) The difference in average velocities at lower valve lifts is negligible between both liners across pressure differences, but at higher valve lifts, for the case of 150mmH₂O, 12.9% and 14.28% were recorded at 4mm and 5.4mm valve lifts, respectively. Meanwhile, a difference of 15.67% was recorded at 5.4mm valve lift for 600 mmH₂O case.
- iii) Plane 2 shows the most difference in terms of Average TKE, with the curve cylinder producing more average TKE, up to 11.44% and 10.09% for 150mmH₂O and 600mmH₂O, respectively. Meanwhile, at higher valve lift, the differences of 6% to 7% in average TKE were recorded for both liners favoring curve cylinder liners.

- iv) The air rotational strength increases as air jets enter cylinder liners assisted by the curve wall towards the piston crown thus spreading into central region of cylinder and can be seen across all cases especially in higher valve lift and pressure difference.
- v) The tumble ratio produced within curve cylinder was found to be significantly higher compared to slider cylinder liner and noticeable starting at lower valve lift, with difference of 5.99% and 7.86%. Moreover, the larger differences of 17.03% and 11.04% were found at higher valve lift (5.4mm) for 150mmH₂O and 600mmH₂O, respectively.

Acknowledgement

This project was supported by Universiti Teknologi PETRONAS, Malaysia, under Yayasan Universiti Teknologi PETRONAS (YUTP) Grant, cost centre 015LC0-127.

References

- [1] Murali, Krishna B., and J. M. Mallikarjuna. "Effect of engine speed on in-cylinder tumble flows in a motored internal combustion engine-an experimental investigation using particle image velocimetry." (2011): 1-14. <https://doi.org/10.36884/jafm.4.01.11895>
- [2] Yang, Xiaofeng, Tang-Wei Kuo, Orgun Guralp, Ronald O. Grover Jr, and Paul Najt. "In-Cylinder Flow Correlations between steady flow bench and motored engine using computational fluid dynamics." *Journal of Engineering for Gas Turbines and Power* 139, no. 7 (2017): 072802. <https://doi.org/10.1115/1.4035627>
- [3] EL-Adawy, Mohammed, M. R. Heikal, A. Rashid A Aziz, M. I. Siddiqui, Hasanain A. Abdul Wahhab, and Hasanain A. Hasanain A. "Tumble Motion Evolution for GDI Engine Using Particle Image Velocimetry (PIV)." *Journal of Mechanical Engineering (JMEchE)* 1 (2018): 191-201.
- [4] Krishna, B. Murali, and J. M. Mallikarjuna. "Tumble flow analysis in an unfired engine using particle image velocimetry." *International Journal of Mechanical and Mechatronics Engineering* 3, no. 6 (2009): 706-711.
- [5] Davario, Alessandro, and Vincenzo Di Lella. "Experimental Study of a Flow into an Engine Cylinder Using PIV." (2017).
- [6] Heim, Douglas, and Jaal Ghandhi. "A detailed study of in-cylinder flow and turbulence using PIV." *SAE International Journal of Engines* 4, no. 1 (2011): 1642-1668. <https://doi.org/10.4271/2011-01-1287>
- [7] Baum, E., B. Peterson, C. Surmann, D. Michaelis, B. Böhm, and A. Dreizler. "Investigation of the 3D flow field in an IC engine using tomographic PIV." *Proceedings of the Combustion Institute* 34, no. 2 (2013): 2903-2910. <https://doi.org/10.1016/j.proci.2012.06.123>
- [8] El-Adawy, Mohammed, Morgan R. Heikal, A. Rashid A. Aziz, Muhammad I. Siddiqui, and Shahzad Munir. "Characterization of the inlet port flow under steady-state conditions using piv and pod." *Energies* 10, no. 12 (2017): 1950. <https://doi.org/10.3390/en10121950>
- [9] Shafie, AM Mohd, M. T. Musthafah, M. S. Ali, and Rosli A. Bakar. "Intake analysis on four-stroke engine using CFD." *ARPN Journal of Engineering and Applied Sciences* 10, no. 17 (2015).
- [10] Pandey, K. M., and Bidesh Roy. "CFD analysis of intake valve for port petrol injection SI engine." *Global Journal of Researches in Engineering* 12, no. 5 (2012): 13-19.
- [11] Gundmalm, Stefan. "CFD modeling of a four stroke SI engine for motorcycle application." *s Interneta* 15 (2009).
- [12] Belkebir, Saliha Mohammed, Benyoucef Khelidj, and Miloud Tahar-Abbes. "Study of the Combustion Process of a Homogeneous Charge Compression Ignition (HCCI) Engine and a Partially Premixed Combustion (PPC) Mode of a Compression Ignition Engine Using Natural Gas as an Alternative Fuel." *Journal of Advanced Research in Fluid Mechanics and Thermal Sciences* 84, no. 2 (2021): 98-115. <https://doi.org/10.37934/arfmts.84.2.98115>
- [13] Yahaya, N., A. M. M. Ismail, N. A. Sabrin, Nurrul Amilin, A. Nalisa, Ilya Izyan, and Y. Ramli. "Investigation of Whitcomb's Winglet Flow Behaviour using PIV and FLUENT." *Journal of Advanced Research in Fluid Mechanics and Thermal Sciences* 13, no. 1 (2015): 22-28.
- [14] Ismail, Ainaa Maya Munira, Fazila Mohd Nawawi, and Jamaludin Md Sheriff. "Flow Pattern and Particle Contamination in Fluid Flow through Mitre Bend." *Journal of Advanced Research in Fluid Mechanics and Thermal Sciences* 45, no. 1 (2018): 128-140.
- [15] Zahari, Nazirul Mubin, Mohd Hafiz Zawawi, Lariyah Mohd Sidek, Fei Chong Ng, Mohamad Aizat Abas, Farah Nurhikmah, and Muhammad Naqib Nashrudin. "Discrete Phase Modelling of Sediment Transport and Scouring of Suspended Particles in Dam Spillway." *Journal of Advanced Research in Fluid Mechanics and Thermal Sciences* 88, no. 2 (2021): 38-49. <https://doi.org/10.37934/arfmts.88.2.3849>

- [16] Scott, Blane, Christopher Willman, Richard Stone, Giuseppe Virelli, Rachel Magnanon, and David Richardson. *Novel metrics for validation of PIV and CFD in IC engines*. No. 2019-01-0716. SAE Technical Paper, 2019. <https://doi.org/10.4271/2019-01-0716>
- [17] Pairan, Mohamad Rasidi, Sharul Azmir Osman, Ahmad Nabil Md Nasir, Nur Hazirah Noh, Mohd Hizwan Mohd Hisham, Adjah Naqkiah Mazlan, Hanifah Jambari, and Muhamad Afzamiman Aripin. "The blockage ratio effect to the spray performances." *Journal of Advanced Research in Fluid Mechanics and Thermal Sciences* 95, no. 1 (2022): 99-109. <https://doi.org/10.37934/arfmts.95.1.99109>
- [18] Jamil, Abdullah, Masri B. Baharom, and A. Rashid A. Aziz. "IC engine in-cylinder cold-flow analysis—A critical review." *Alexandria Engineering Journal* 60, no. 3 (2021): 2921-2945. <https://doi.org/10.1016/j.aej.2021.01.040>
- [19] Heywood, John B. *Internal combustion engine fundamentals*. McGraw-Hill Education, 2018.
- [20] El-Adawy, Mohammed, M. R. Heikal, A. Rashid A. Aziz, M. I. Siddiqui, and Hasanain A. Abdul Wahhab. "Experimental study on an IC engine in-cylinder flow using different steady-state flow benches." *Alexandria Engineering Journal* 56, no. 4 (2017): 727-736. <https://doi.org/10.1016/j.aej.2017.08.015>
- [21] Mohammed, Salah E., M. B. Baharom, and A. Rashid A. Aziz. "Performance and combustion characteristics of a novel crank-rocker engine." *Journal of Mechanical Science and Technology* 31 (2017): 3563-3571. <https://doi.org/10.1007/s12206-017-0643-x>
- [22] Jamil, Abdullah, Masri B. Baharom, and Abd Rashid B. Abd Aziz. "In-Cylinder Cold-Flow Analysis—A Comparison of Crank-Slider Engine and Crank-Rocker Engine'." *Journal Européen des Systèmes Automatisés* 55, no. 2 (2022). <https://doi.org/10.18280/jesa.550210>
- [23] Tariq, Adeel, Khurram Altaf, Ahmad Majdi Abdul Rani, and Masri Baharom. "Study of Heat Transfer Attributes of Custom Fins for CrankRocker Engine Block using ANSYS." *Journal of Advanced Research in Fluid Mechanics and Thermal Sciences* 62, no. 2 (2019): 235-243.
- [24] Mohammed, Salah Eldin, Masri Baharom, and Abdul Rashid Abdul Aziz. "Comparative analysis of two proposed models of connecting rods for crank-rocker engines using finite element method." In *MATEC Web of Conferences*, vol. 13, p. 02019. EDP Sciences, 2014. <https://doi.org/10.1051/mateconf/20141302019>
- [25] Kardan, Ramtin, M. B. Baharom, Salah E. Mohammed, A. Rashid A. Aziz, and Firmansyah Firmansyah. "The effect of engine throttle position on the performance characteristics of a crank-rocker engine fitted with a conventional cylinder head." In *AIP Conference Proceedings*, vol. 2035, no. 1. AIP Publishing, 2018. <https://doi.org/10.1063/1.5075549>
- [26] Krastev, Vesselin Krassimirov, Luca Silvestri, and Giacomo Falcucci. "A modified version of the RNG k- ϵ turbulence model for the scale-resolving simulation of internal combustion engines." *Energies* 10, no. 12 (2017): 2116. <https://doi.org/10.3390/en10122116>
- [27] El Adawy, Mohammed, M. R. Heikal, A. Rashid A Aziz, S. Munir, and M. I. Siddiqui. "Effect of boost pressure on the in-cylinder tumble-motion of GDI engine under steady-state conditions using Stereoscopic-PIV." *Journal of Applied Fluid Mechanics* 11, no. 3 (2018): 733-742. <https://doi.org/10.29252/jafm.11.03.28506>
- [28] Hatschbach, Petr, Oldřich Vítek, and Radek Tichánek. "In-cylinder flow characterization using vorticity based parameters." *MECCA Journal of Middle European Construction and Design of Cars* 18, no. 1 (2021): 11-11. <https://doi.org/10.14311/mecdc.2021.01.03>
- [29] El Adawy, Mohammed, M. R. Heikal, and A. Rashid A Aziz. "Experimental investigation of the in-cylinder tumble motion inside GDI cylinder at different planes under steady-state condition using stereoscopic-PIV." *Journal of Applied Fluid Mechanics* 12, no. 1 (2019): 41-49. <https://doi.org/10.29252/jafm.75.253.28885>